Biochimica et Biophysica Acta, 1152 (1993) 49–60

BBAMEM 76081

Thermodynamic stability and osmotic sensitivity of small unilamellar phosphatidylcholine vesicles

Brigitte Lerebours [a], Ernst Wehrli [b] and Helmut Hauser [a,*]

[a] *Laboratorium für Biochemie, Laboratorium für Elektronenmikroskopie, Eidgenössische Technische Hochschule, ETH Zentrum, CH-8092 Zürich (Switzerland) and* [b] *Institut für Zellbiologie, Laboratorium für Elektronenmikroskopie, Eidgenössische Technische Hochschule, ETH Zentrum, CH-8092 Zürich (Switzerland)*

(Received 6 April 1993)

Key words: Phosphatidylcholine; Unilamellar vesicle; Osmotic sensitivity; Salt gradient; Thermodynamic stability

Evidence is presented to show that small unilamellar phosphatidylcholine vesicles with a diameter of approx. 20 nm are osmotically sensitive. Such vesicles respond to osmotic pressure by swelling or shrinking depending on the direction of the applied salt gradient. This is true for small unilamellar vesicles of egg phosphatidylcholine and dimyristoylphosphatidylcholine below and above their crystal-to-liquid crystal transition temperature. At the transition temperature the vesicles are osmotically insensitive due to the increased bilayer permeability resulting in rapid dissipation of salt gradients. Positive salt gradients produce shrinking and collapse of spherical phospholipid vesicles to disks. Shrinking of vesicles is associated with H_2O and solute efflux, but only limited solute influx. Clustering of lipid molecules in the bilayers of the resulting disks can be detected by EPR spin labeling. Negative salt gradients produce swelling of vesicles which is associated with H_2O and solute influx. Our experiments are consistent with an osmotically perturbed bilayer. In the presence of osmotic gradients the influx and efflux of H_2O is coupled with the movement of ions and small molecules which in the absence of salt gradients or osmotic stress cannot pass the phospholipid bilayer. However, during osmotically induced shrinking and swelling of SUV the integrity of the phospholipid bilayer is maintained to the extent that vesicles do not break, and therefore equilibration between external medium and vesicle cavity does not take place.

Introduction

Small unilamellar phospholipid vesicles (SUV) of diameter smaller than 50 nm produced by ultrasonication have been shown to be under tension. It has been demonstrated for SUV of phosphatidylcholines by using several physical methods, e.g., high-resolution NMR, that the phospholipid molecules on the inner monolayer of the bilayer are packed under stress [1–4] and therefore the surface tension of SUV exceeds that of planar bilayers. SUV of a diameter smaller than 50 nm are therefore thermodynamically unstable or metastable.

The question arises as to how small unilamellar phospholipid vesicles, which are already under stress, respond to osmotic pressure. Johnson and Buttress [5] reported that SUV consisting of either charged or uncharged lipids are osmotically insensitive. In contrast, large unilamellar phosphatidylcholine vesicles [6] and very large, thin-walled, probably oligolamellar vesicles have been described as osmotically active [7]. In a more recent study using stopped-flow light-scattering the conclusion was arrived at that only lipid vesicles with a diameter greater than about 80 nm give an osmotic response, while vesicles smaller than this were described as nondeformable [8].

The conclusion that SUV smaller than approx. 80 nm are osmotically insensitive is unexpected from a theoretical point of view and prompted the study presented in this paper. The effect of positive and negative salt gradients on SUV with a minimum radius of curvature has been determined using freeze-fracture electron microscopy, EPR spin labeling and fluorescence spectroscopy. We can show that in the presence of negative salt gradients, i.e., with the salt concentration of the vesicle cavity exceeding that of the dispersion medium, the excess osmotic pressure of the vesicle cavity causes swelling of the SUV, while the reverse

* Corresponding author.

Abbreviations: CAT 16, 4-(*N,N*-dimethyl-*N*-hexadecylammonio)-2,2,6,6-tetramethylpiperidine-1-oxyl iodide; DMPC, 1,2-dimyristoyl-*rac*-glycero-3-phosphocholine; EPC, egg phosphatidylcholine; FFEM, freeze-fracture electron microscopy; MLV, multilamellar vesicle(s); SUV, small unilamellar vesicle(s).

situation of positive salt gradients causes the SUV to shrink and eventually to collapse.

Materials and Methods

Materials

Egg phosphatidylcholine (EPC) was purchased from Lipid Products (South Nutfield, Surrey, UK), 4(5)-carboxyfluorescein and ascorbic acid from Fluka (Buchs, Switzerland) and the spin-labeled compounds 4-(*N,N*-dimethyl-*N*-hexadecylammonio)-2,2,6,6-tetramethylpiperidine-1-oxyl iodide (CAT 16) and 4-(*N,N*-dimethyl-*N*-(2-hydroxyethyl)ammonio)-2,2,6,6-tetramethylpiperidine-1-oxyl chloride (Tempocholine) from Molecular Probes (Eugene, OR, USA). 1,2-Dimyristoyl-*rac*-glycero-3-phosphocholine (DMPC) was synthesized by Mr. R. Bertchold (Biochemisches Laboratorium, Bern, Switzerland).

All lipids used were shown to be pure by TLC standards. TLC analyses of lipids were carried out routinely before and after finishing the experiment. Silicagel plates (Kieselgel 60 F_{254}) from Merck (Darmstadt, Germany) were used, 0.5 mg lipid were applied as a 0.8 cm band, and $CHCl_3/CH_3OH$/water (65:25:4, v/v) was used as the solvent. Lipid bands were detected with I_2 vapour. All other chemicals used in this work were of analytical grade.

Methods

Preparation of small unilamellar vesicles (SUV). Crystalline DMPC (10–100 mg) was dissolved in $CHCl_3$ and the solution was taken to dryness in a round-bottom flask by rotary evaporation. The phospholipid film was dried in vacuo for approx. 1 h. The dried phospholipid was dispersed to the desired concentration (5–50 mg/ml) by adding the appropriate volume of either 0.01 M potassium phosphate buffer or 0.01 M Tris buffer adjusted to a pH between 6.8 and 7.2, and repeated vortexing at 30°C for approx. 5 min.

Aliquots (2 ml) of the resulting phospholipid dispersion were immersed in a cooling bath of approx. 5°C, sonicated under N_2 for 45 min using a microtip sonicator (Branson B-30). Titanium particles released from the sonicator tip were removed by centrifugation at $12000 \times g$ for 10 min. If the experiment was not carried out immediately after the preparation, the sonicated lipid dispersions was saturated with N_2 and stored at 4°C.

For the preparation of sonicated DMPC or EPC dispersions labeled with CAT 16, the spin label was added to the phospholipid solution in $CHCl_3$ (phospholipid/spin label, mole ratio approx. 20:1) and the dispersion was made as described above. For the production of SUV of DMPC or EPC containing Tempocholine or carboxyfluorescein entrapped in their aqueous cavity, a buffer containing either 2.5 mM Tempocholine or 50 mM carboxyfluorescein was added to the dry lipid film and the phospholipid dispersion was made as described above. The SUV preparation containing carboxyfluorescein was subjected to gel filtration on Sepharose CL-4B in order to separate external carboxyfluorescein from SUV.

Exposing lipid dispersions to osmotic pressure. For swelling experiments the lipid dispersions were prepared as described above except that salt was added to the buffer used to disperse the dry lipid film. The lipid dispersion (volume v_0) was incubated at the desired temperature for 15 min and diluted with the same volume v_0 of a hypotonic salt solution in the same buffer pre-equilibrated to the same temperature. The resulting mixture was incubated at this temperature for 15 min.

Alternatively, the phospholipid dispersion in either 0.01 M potassium phosphate or 0.01 M Tris buffer was exposed to a salt solution in the same buffer. For this purpose equal volumes of lipid dispersion in buffer and hypertonic salt solution in the same buffer both pre-equilibrated at the desired temperature for 15 min were mixed and the mixture was incubated at the same temperature for 15 min.

Osmotic effects were produced by either exposing phospholipid vesicles to a positive or negative salt gradient ΔC. The salt gradient is defined as $\Delta C = [\text{salt}]_{\text{outside}} - [\text{salt}]_{\text{inside}}$ and is positive if the salt concentration of the external dispersion medium exceeds that of the internal vesicle cavity. Unless stated otherwise salt gradients were produced with LiCl.

Freeze-fracture electron microscopy (FFEM). Aqueous lipid dispersions were frozen from different temperatures using the propane-jet method [9,10] The cryofixed samples were fractured at 123 K and 10^{-6} Pa in a Balzer BAF 300 freeze-etching apparatus. Platinum/carbon replicas were produced and examined in a Philips EM 301 electron microscope operating at 100 kV.

For the size distribution of lipid vesicles the diameter of 200–400 vesicles was measured. Since the angle of incidence of the platinum gun was 45°, the boundary of the platinum shadow of equatorially fractured vesicles dissects the circular image. Only images that fulfill this condition were used in the size analyses which are presented as bar histograms. The error of the vesicle size analyses was estimated to be ± 2 nm and the width of the bars of the histograms was chosen to be 5 nm.

Electron paramagnetic resonance (EPR) spectroscopy. Lipid dispersions were spin-labeled as described above; 30 μl of such a dispersion were cooled to 0°C and diluted with 10 μl 0.5 M sodium ascorbate precooled to 0°C to a final ascorbate concentration of 0.13 M.

The EPR experiments described here make good use of the observation that phosphatidylcholine bilayers are impermeable to sodium ascorbate at 0°C [11]. An ascorbate concentration of 0.13 M instantaneously reduced free Tempocholine molecules present in the dispersion medium of SUV. EPR signal intensities were normalized by setting the intensity measured after the addition of ascorbate equal to 200% (sample volume = 40 μl). Lipid dispersions were then diluted with an equal volume of buffer (sample volume = 80 μl, signal intensity = 100%) or, if osmotic effects were to be measured, with an equal volume of buffer containing the appropriate concentration of salt cooled to 0°C.

Upon exposing aqueous dispersions of SUV labeled with CAT 16 to 0.13 M sodium ascorbate (sample volume = 40 μl) the spin label present in the external layer of the phospholipid bilayer was reduced and the remaining spin label intensity, arising from spin label molecules present in the inner monolayer of the lipid bilayer was taken as 200% and served as reference. If osmotic effects were to be measured, the dispersions were diluted with an equal volume of the appropriate salt solution cooled to 0°C (sample volume = 80 μl) and the intensity of the EPR spectrum observed after dilution was measured.

The line height of the low-field EPR signal was taken as an approximate measure of the signal intensity and changes in the line height of this signal were expressed as % = 200 × (line height ratio sample/reference).

Spin-labeled phospholipid dispersions were filled into 100 μl glass capillaries and cooled to 0°C. Sodium ascorbate and salt solutions both precooled to 0°C were then injected into these glass capillaries and the solutions were thoroughly mixed by aspiration and reinjection. EPR spectra were recorded at 9.2 GHz with a Varian X-band spectrometer (Model E-104A) fitted with a variable temperature control. The temperature was monitored with a thermocouple before and after recording the spectrum and was accurate to ±0.5°C.

Fluorescence spectroscopy. Fluorescence spectroscopy was applied to SUV of phosphatidylcholine containing carboxyfluorescein at self-quenching concentrations (approx. 50 mM) entrapped in their internal cavity. Leakage of the carboxyfluorescein molecules was detected by an increase in the fluorescence intensity. Fluorescence intensities were measured with an Aminco SPF-500 spectrofluorimeter (excitation at 480 nm, band pass 4 nm; emission at 515 nm, band pass 1 nm). The sample cell was thermostatted at 35°C with a Lauda RC3 thermostat. Over the concentration range of carboxyfluorescein from 10^{-8} to $3 \cdot 10^{-5}$ M the fluorescence intensity was linearly related to the carboxyfluorescein concentration.

Results

Thermodynamic stability of sonicated dimyristoylphosphatidylcholine dispersions. Particle size analysis

FFEM was used to derive the average size and size distribution of sonicated DMPC dispersions and to study the effect of positive and negative salt gradients. Representative electron micrographs of freeze-fractured preparations of sonicated phosphatidylcholine dispersions are shown in Fig. 1A, C, E and G. The effect of salt gradients, mostly as LiCl gradients is depicted in Fig. 1B, D, F and H. The bar histograms shown in Figs. 2 and 3 were derived from electron micrographs such as those shown in Fig. 1.

The size distribution of small unilamellar DMPC vesicles is adequately described by the Weibull extreme probability distribution. This function was used before to describe the size distribution of SUV consisting of EPC and dipalmitoylphosphatidylethanolamine [12]. The Weibull distribution is given by the following equations:

$$f(\Phi) = \frac{\delta}{\eta}\left(\frac{\Phi - \Phi_0}{\eta}\right)^{\delta-1} \exp\left[-\left(\frac{\Phi - \Phi_0}{\eta}\right)^{\delta}\right]$$

and

$$\Phi_{max} = \Phi_0 + \eta\left(\frac{\delta - 1}{\delta}\right)^{1/\delta}$$

$$E = \Phi_0 + \eta\left(\frac{1}{\delta}\right)!$$

$$D = \eta\left\{\left(\frac{2}{\delta}\right)! - \left[\left(\frac{1}{\delta}\right)!\right]^2\right\}^{1/2}$$

where Φ_o, Φ_{max} are the lower size limit and the most probable size, respectively, E is the expectancy or mean value of the vesicle diameter and D the dispersion of the Weibull distribution. δ and η are fitting parameters.

As an example, the Weibull distribution fitted to the full bars of Fig. 2A by a least-squares procedure is included in this figure. The vesicle size analysis derived from this approach is summarized in Table I. As evident from this table and Fig. 2, Φ_{max} of a frehsly prepared DMPC dispersion is 20.0 ± 0.5 nm, and this value is independent of the phospholipid concentration in the range 5–50 mg/ml. Similar values for Φ_{max} were obtained for DMPC dispersions below and above the phospholipid transition temperature. Storing the DMPC dispersion at low temperatures (0–4°C) for up to 8 days had little effect on the average size and size distribution (Table I). For instance, storing a DMPC dispersion at 4°C for 8 days shifted the first maximum to 25 nm with a second maximum appearing at about

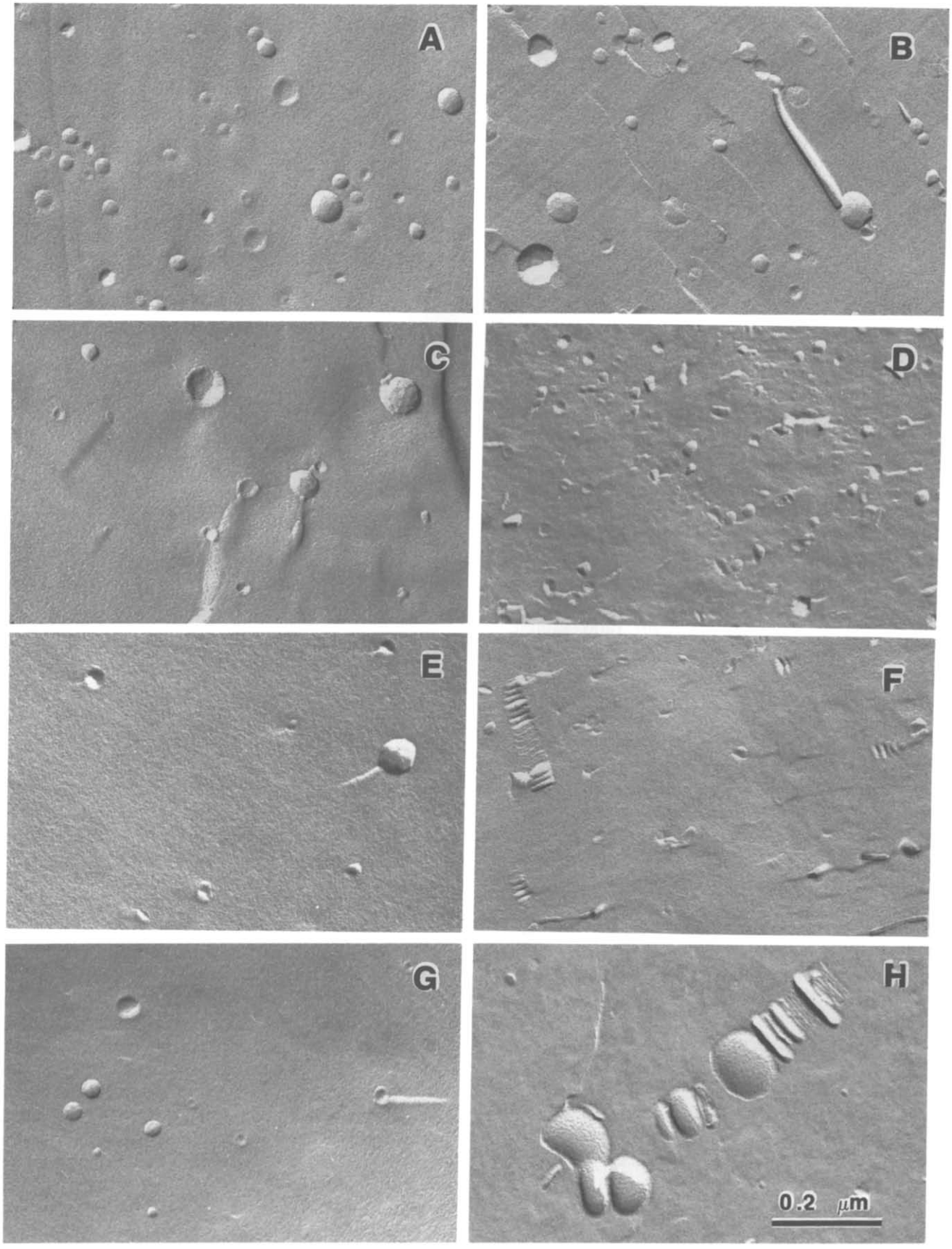
A
B
C
D
E
F
G
H
0.2 μm

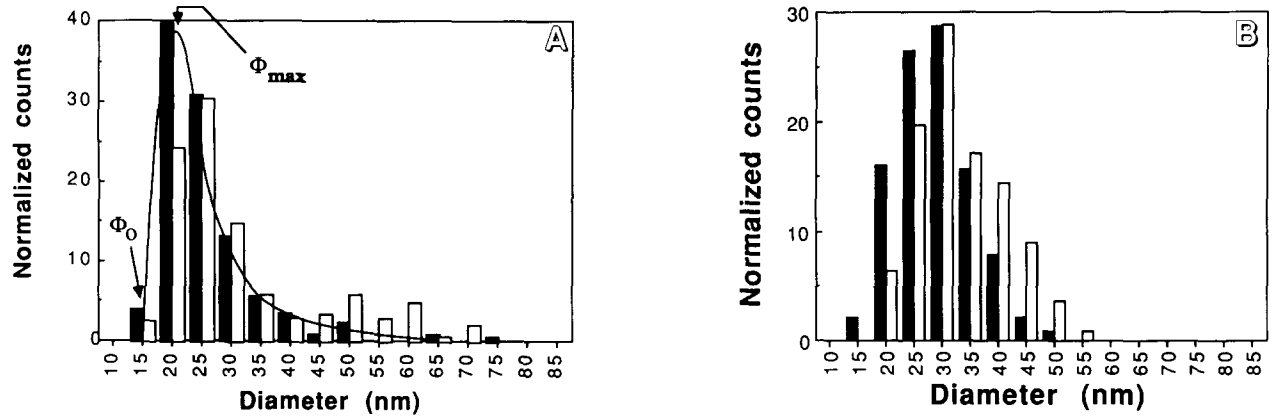

Fig. 2. Bar histograms derived from FFEM of sonicated DMPC dispersions in 0.01 M Tris buffer (pH 7). (A) Bar histogram of a sonicated dispersion of 50 mg lipid/ml stored at 0–4°C for 1 day (closed bars) and 8 days (open bars). The solid line represents the Weibull distribution fitted to the bar histogram of the one-day-old sample. The parameters of the Weibull distribution thus derived were: $\Phi_o = 14.9$ nm, $\Phi_{max} = 20.5$ nm, $E = 23.6$ nm, $D = 5.4$ nm. (B) Bar histograms of a sonicated dispersion (5 mg lipid/ml) stored at room temperature for 1 day (closed bars) and 8 days (open bars).

TABLE I

Parameters of Weibull distributions fitted to the bar histograms derived from FFEM

Sonicated dispersions of DMPC (5 mg lipid/ml) in Tris buffer (pH 7) were prepared as described in Materials and Methods. Unless stated otherwise the dispersions were incubated at 0°C for 30 min and then frozen from this temperature. The effect of lipid concentration, temperature, storage time and increased salt concentrations on the vesicle size distribution of DMPC was studied.

Experimental conditions	Φ_o (nm)	Φ_{max} (nm)	E (nm)	D (nm)
Effect of concentration				
at 5 mg lipid/ml	14.9	19.6	23.0	5.3
at 50 mg lipid/ml	14.9	20.5	23.6	5.4
Effect of temperature				
at 0°C	15.0	20.6	24.8	6.5
at 20°C	15.0	21.4	26.6	7.8
at 40°C	14.9	19.6	23.0	5.3
Effect of storage				
at 0°C for 1 day	14.9	20.5	23.6	5.4
at 0°C for 8 days	15.0	21.4	26.2	7.8
at 23°C for 1 day	13.3	27.4	28.6	6.6
at 23°C for 8 days	18.9	29.4	33.2	8.1
Effect of salt concentration				
SUV prepared in buffer	15.0	20.6	24.8	6.5
SUV prepared in LiCl 1 M	14.5	20.6	22.4	4.3
SUV prepared in LiCl 3 M	8.8	17.9	19.9	5.6

50 nm (cf. open bar histogram of Fig. 2A). However, storing DMPC dispersions at temperatures which are at or close to the phospholipid order–disorder transition temperature $T_c = 23$°C [13,14] produced significant changes in the vesicle size and size distribution. As shown in Fig. 2B storing a sonicated DMPC dispersion at 23°C for 8 days caused a shift of the bar histogram to larger diameters and corresponding changes in the parameters of the Weibull distribution (Table I). Not only did Φ_{max} and E increase, but also the value for the dispersion of the Weibull distribution.

The effect of osmotic pressure on small unilamellar phosphatidylcholine vesicles

Freeze-fracture electron microscopy. SUV of DMPC of the size described above respond to positive and negative salt gradients, with shrinking and swelling, respectively. Exposing DMPC SUV to positive salt gradients $\Delta C > 1$ M caused shrinkage of the vesicles both below and above the transition temperature T_c (Fig. 1D, F), but not at the transition temperature (Fig. 1B). At 0°C both single and stacked disks prevailed (Fig. 1F), the thickness of which was 10 ± 2 nm. This is about double the bilayer thickness indicating that the observed disks are collapsed SUV. At temperatures above T_c, e.g., at 40°C, the shrinking of the vesicles is

Fig. 1. Electron micrographs of freeze-fractured preparation of phosphatidylcholine dispersions. Aliquots of the dispersions (50 μl) of SUV in 0.01 M Tris buffer (pH about 7.0) were equilibrated for 15 min at a certain temperature designated as the incubation temperature T_i. Then 50 μl of buffer solution with or without salt previously stabilized at the same temperature T_i were added and the mixture was equilibrated at T_i for 15 min and jet-frozen. SUV of DMPC (5 mg lipid/ml) and EPC (10 mg lipid/ml) were prepared as described in Materials and Methods and treated as described above. The electron micrographs A, C, E and G show dispersions of SUV in the absence of a salt gradient ($\Delta C = 0$) jet-frozen from different temperatures while those of B, D, F and H show the same dispersions in the presence of a positive salt gradient. A and B: SUV of DMPC, T_i = room temperature, $\Delta C = 0$ M and $\Delta C = 2.1$ M of KCl, respectively. C and D: SUV of DMPC, $T_i = 40$°C, $\Delta C = 0$ M and $\Delta C = 3$ M of LiCl, respectively. E and F: SUV of DMPC, $T_i = 0$°C, $\Delta C = 0$ M and $\Delta C = 1$ M of LiCl, respectively. G and H: SUV of EPC, T_i = room temperature, $\Delta C = 0$ M and $\Delta C = 3$ M of LiCl, respectively.

not as well documented as at 0°C (cf. Fig. 1D and 1F). This may be due to difficulties in efficiently freezing phospholipid dispersions from 40°C. In support of this explanation is the effect of positive salt gradients on sonicated EPC dispersions at room temperature at which EPC bilayers are in the liquid crystalline state. Similar to DMPC vesicles at 0°C (Fig. 1F), shrinkage of EPC-SUV occurred under these conditions and also stacking of partly flattened vesicles and disks resulting from the total collapse of the original spherical vesicles (Fig. 1G and 1H). A visual comparison of the size of the flattened vesicles and disks with that of the original spherical vesicles (cf. Fig. 1G and 1H) indicates that massive vesicle fusion occurs under these conditions.

The dimensions of the disks derived from FFEM can be converted to the diameter of the parent spherical vesicles as shown in the Appendix. In this way a vesicle size distribution is derived from electron micrographs such as those of Fig. 1F and H and the size distribution derived from disks may be compared with that of the parent spherical vesicles. Results thus obtained are summarized in Fig. 3. This figure shows that the dimensions derived from isolated, single disks are consistent with those of the original vesicles indicating that the observed disks indeed represent collapsed vesicles (cf. full and hatched bars of Fig. 3A–C). In contrast, the bar histograms derived from stacked disks are all shifted to larger vesicle sizes (cf. steepled bars in Fig. 3A–C) indicating that osmotically induced shrinkage is accompanied by vesicle fusion. A comparison of Fig. 3A and B suggests that the extent of stacking and hence of aggregation/fusion decreased with increasing osmotic pressure or salt concentration in the dispersion medium. At $\Delta C = 1$ M about 80% of the disks were present in stacks while at $\Delta C = 3$ M this number was reduced to 50%. Whenever possible Weibull distributions were fitted to the bar histograms and the parameters of these Weibull distributions are summarized in Table II. These parameters lend support to the qualitative interpretation of the electron microscopy results discussed above. In the presence of negative salt gradients $\Delta C < 0$, DMPC-SUV swelled as evident from FFEM (data not shown) and Weibull distributions fitted to the bar histograms derived from FFEM (Table II).

EPR spectroscopy. SUV of DMPC and EPC were loaded with Tempocholine, cooled to 0°C, exposed to excess sodium ascorbate (0.13 M) and then confronted with salt gradients. The EPR spectrum of Tempocholine entrapped in the vesicle cavity is shown as Fig. 4B. Exposing SUV to positive LiCl gradients produced a decrease in the EPR signal intensity which was nonlinear with ΔC (Fig. 4). About 80% of the entrapped Tempocholine was reduced in the presence of a LiCl gradient of $\Delta C = 0.5$–1 M. A similar trend was observed when EPC vesicles loaded with Tem-

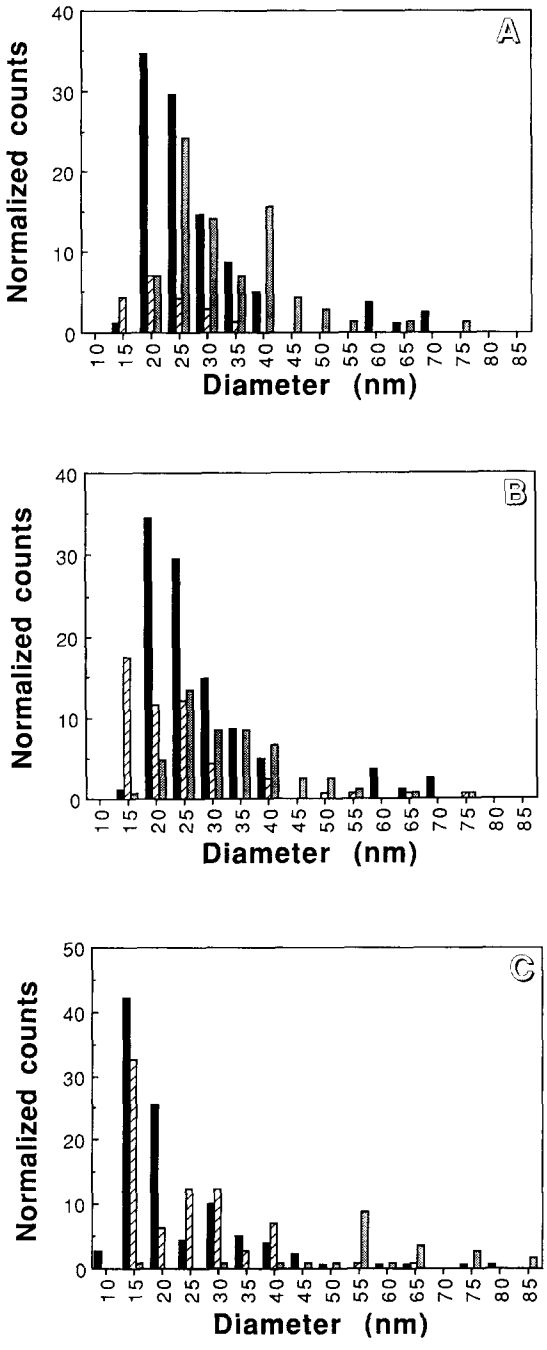

Fig. 3. Bar histograms derived from FFEM of sonicated phosphatidylcholine dispersions. (A) DMPC (5 mg lipid/ml) was dispersed in 0.01 M Tris buffer (pH 7), incubated at 0°C and exposed to a positive LiCl gradient of $\Delta C = 1$ M at 0°C for 30 min before propane-jet freezing of the dispersion. Cross-hatched bars: the dimensions of isolated disks were measured in electron micrographs and converted to diameters of spherical vesicles using the approach described in the Appendix. Steepled bars: the dimensions of stacked disks were transformed to diameters of spherical vesicles. For comparison, the bar histogram of the same sonicated DMPC dispersion in the absence of salt gradient ($\Delta C = 0$) is included (solid bars). (B) The same dispersion as in A was exposed to a positive LiCl gradient of $\Delta C = 3$ M at 0°C for 30 min. (C) EPC (10 mg lipid/ml) was dispersed in 0.01 M Tris buffer (pH 7) and exposed to a positive LiCl gradient of $\Delta C = 3$ M at room temperature for 30 min before propane-jet freezing of the dispersion. In (B) and (C), the same key to the bars was used as in (A).

TABLE II

Parameters of Weibull distributions fitted to bar histograms derived from FFEM

Sonicated dispersions of DMPC (5 mg lipid/ml) were prepared either in Tris buffer (pH 7) or in Tris buffer containing [LiCl] = 1 M and [LiCl] = 3 M as described in Materials and Methods. The effect of positive and negative salt gradients was studied at 0°C.

Experimental conditions	Φ_o (nm)	Φ_{max} (nm)	E (nm)	D (nm)
SUV prepared in buffer				
$\Delta C = 0$	15.0	20.6	24.8	6.5
$\Delta C = 1$ M (stacked disks)	19.9	24.6	36.3	13.3
$\Delta C = 3$ M (stacked disks)	14.9	24.9	61.5	39.6
SUV prepared in LiCl 1 M				
$\Delta C = 0$	14.5	20.6	22.4	4.3
$\Delta C = -0.5$ M	10.0	22.0	22.6	4.9
SUV prepared in LiCl 3 M				
$\Delta C = 0$	8.8	17.9	19.9	5.6
$\Delta C = -0.75$ M	5.6	20.9	20.8	4.9
$\Delta C = -1.5$ M	12.2	24.0	24.5	4.8

pocholine were exposed to LiCl gradients. These experiments were carried out at 0°C and hence DMPC was in the gel state while EPC was liquid crystalline. The data in Fig. 4 suggest that SUV of DMPC in the gel state are slightly more leaky than SUV of EPC in the liquid crystalline state.

SUV of DMPC labeled with CAT 16 were exposed to sodium ascorbate (0.13 M) at 0°C so that CAT 16 molecules located in the outer monolayer of the bilayer were reduced. The remaining EPR signal intensity arises therefore from CAT 16 molecules located in the inner monolayer of the bilayer. Subjecting the vesicles to a positive LiCl gradient of $\Delta C = 1$ M reduced the EPR signal intensity to 50% (Fig. 5). No further reduction of the EPR signal intensity was observed as the LiCl gradient was increased to $\Delta C = 6$ M. When sodium cholate was added to such a dispersion to a final phospholipid/cholate mole ratio of 0.5 all CAT 16 molecules were reduced as would be expected after solubilization of the DMPC vesicles to mixed micelles in the presence of excess bile salt (data not shown). Fig. 5 also illustrates (see open triangles) that even in the absence of ascorbate the shrinkage of SUV of DMPC induced by positive salt gradients is accompanied by a loss of the EPR signal intensity. The EPR signal appears to decrease with increasing LiCl gradient reaching a value of approx. 75% at $\Delta C = 6$ M.

The effects of negative LiCl gradients on SUV of DMPC prepared in buffer containing 4 M LiCl were monitored with Tempocholine entrapped in the vesicle cavity or CAT 16 inserted in the DMPC bilayer. The results of positive and negative LiCl gradients are summarized in Fig. 6A and B, respectively. In both sets of EPR experiments depicted in Fig. 6 maximum signal intensities were observed at $\Delta C = -1.5$ M suggesting that the vesicle cavities are solute-depleted under these conditions. A similar result was reported for multilamellar EPC vesicles [15]. Vesicles containing high concentrations of LiCl entrapped in their cavity did shrink when exposed to positive LiCl gradients $\Delta C > 0$, but did not collapse entirely as evident from FFEM (data not shown). As a result it was not possible to derive their original vesicle diameter from the dimensions of the partially collapsed vesicles using the approach described in the Appendix. FFEM indicates that most of the shrunk vesicles were isolated, i.e., stacking was a minor event in this case (data not shown).

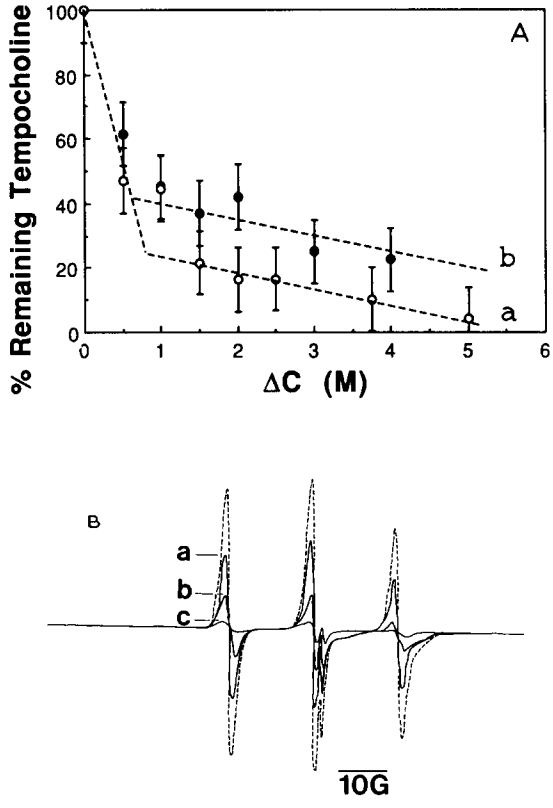

Fig. 4. (A) EPR signal intensities of Tempocholine as a function of a positive LiCl gradient. SUV of DMPC (a) and EPC (b) at 10 mg lipid/ml were prepared in 0.01 M Tris buffer (pH 7) containing 2.5 mM Tempocholine. The lipid dispersion was cooled to approx. 0°C, the external Tempocholine was reduced by adding sodium ascorbate to a final concentration of 0.13 M and the EPR spectrum was recorded. To this dispersion an equal volume of buffer with or without LiCl was added and the effect of positive LiCl gradients on the signal intensity of the EPR spectrum was determined. (B) Original EPR spectrum (dashed) arising from Tempocholine (2.5 mM) entrapped in SUV of DMPC; the EPR spectrum was obtained after the addition of 0.13 M sodium ascorbate with its signal intensity corresponding to 200%. All other EPR spectra (solid lines) were obtained after diluting the lipid dispersion with an equal volume of buffer (a), of buffer containing LiCl so that $\Delta C = 1$ M (b) and $\Delta C = 5$ M (c). The signal intensities recorded after dilution were standardized against the signal intensity of the undiluted sample.

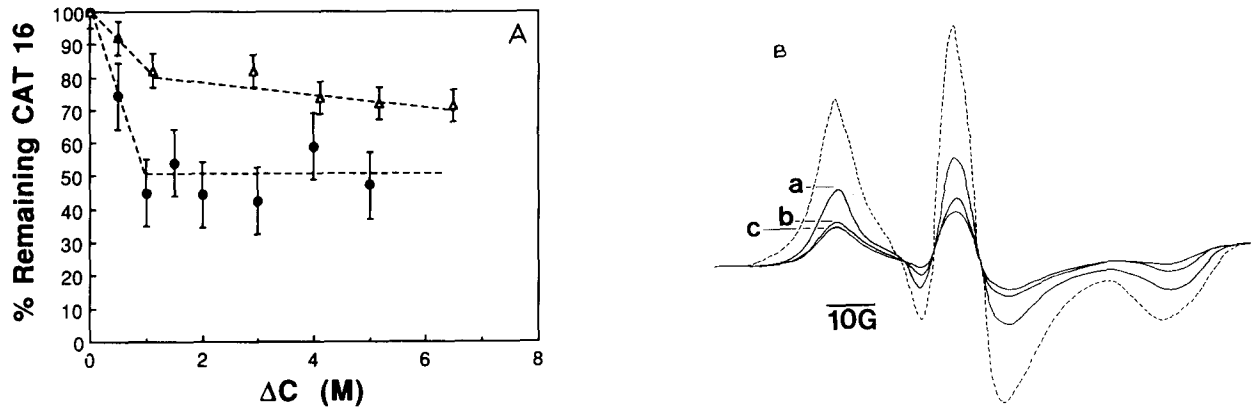

Fig. 5. (A) Reduction of CAT 16 incorporated in the bilayers of SUV of DMPC by excess sodium ascorbate as a fuction of positive LiCl gradients. Sonicated dispersions of DMPC (10 mg lipid/ml) labeled with CAT 16 were prepared in 0.01 M Tris (pH 7) as described in Materials and Methods. The phospholipid dispersions were cooled to 0°C, sodium ascorbate was added to a final concentration of 0.13 M and the EPR spectrum was recorded. Its signal intensity was set equal to 200%. The phospholipid dispersion was diluted with an equal volume of buffer with or without LiCl and the effect of increasing LiCl gradients on the EPR signal intensity was measured (full circles). The same series of experiments was repeated except that no sodium ascorbate was added (open triangles). (B) Original EPR spectrum of CAT 16 incorporated in bilayers of DMPC SUV at a phospholipid/spin label mole ratio of 20:1. The spectrum was recorded after the addition of Na^+ ascorbate to a final concentration of 0.13 M at 0°C (dashed line) and its signal intensity was set equal to 200%. All other EPR spectra (solid lines) were obtained after diluting the phospholipid dispersion with an equal volume of buffer (a) and with an equal volume of buffer containing LiCl so that $\Delta C = 1.5$ M (b) and $\Delta C = 5$ M (c). The signal intensities recorded after dilution were standardized against the signal intensity of the undiluted sample.

With negative gradients a significant reduction of both spin labels was observed; the EPR signal intensities dropped to 50–60% (Fig. 6A and B).

Fluorescence spectroscopy. Fig. 7 illustrates the effect of positive LiCl gradients on SUV of DMPC containing carboxyfluorescein entrapped in the vesicle cavity at self-quenching concentration (50 mM). Positive LiCl gradients cause carboxyfluorescein molecules to escape from the vesicle cavity. This carboxyfluorescein release is indicated by a fluorescence intensity increase. Indeed with increasing LiCl gradients and hence osmotic pressure the fluorescence intensity increased continuously reaching a plateau at ΔC approx. 1.5 M. The dashed line represents the maximum carboxyfluorescein concentration of $2.5 \cdot 10^{-7}$ M which was calculated from the known concentration of DMPC and the average vesicle diameter of 20 nm, assuming a bilayer thickness of 4 nm and a mean molecular area of 0.50 nm^2 [16] (cf. Fig. 7). The data in this figure indicate that at LiCl gradients $\Delta C > 1.5$ M all carboxyfluorescein molecules are released into the bulk aqueous medium. This result was obtained at 35°C, i.e., with DMPC in the liquid crystalline state. When the fluorescence experiments were performed with DMPC vesi-

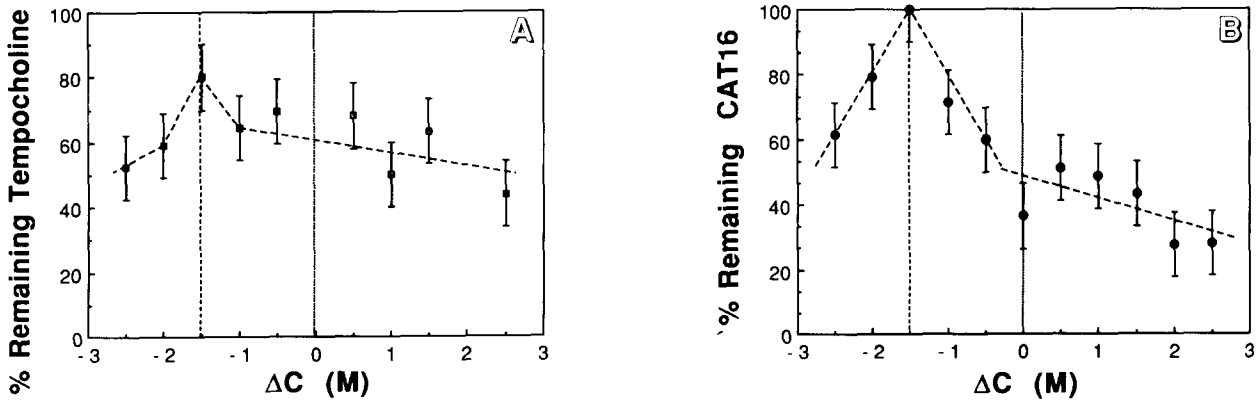

Fig. 6. Reduction of Tempocholine and CAT 16 in SUV of DMPC as a function of positive and negative LiCl gradients. Sonicated dispersions of DMPC (10 mg lipid/ml) were prepared in 0.01 M Tris buffer (pH 7) containing 4 M LiCl and 2.5 mM Tempocholine (A). Alternatively sonicated dispersions of DMPC were made containing CAT 16 in the DMPC bilayer (DMPC/spin label mole ratio = 20) under otherwise the same experimental conditions (B). To both phospholipid dispersions cooled to 0°C sodium ascorbate was added to a final concentration of 0.13 M. EPR spectra were recorded at 0°C and the EPR signal intensity observed after the addition of ascorbate was set equal to 200%. The signal intensities measured after diluting the phospholipid dispersion with an equal volume of buffer containing different LiCl concentrations were standardized against the signal intensity of the undiluted sample. Positive and negative salt gradients of LiCl were applied by diluting the phospholipid dispersion with an equal volume of buffer containing more ($\Delta C > 0$) and less ($\Delta C < 0$) than 4 M LiCl, respectively.

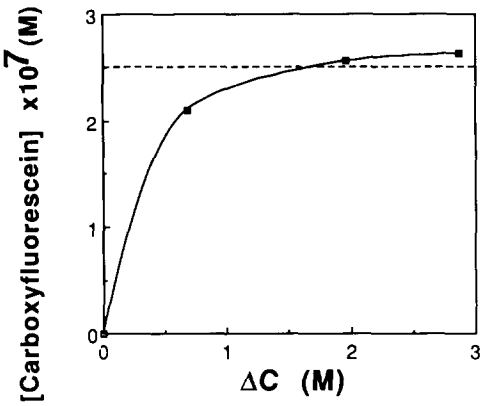

Fig. 7. Fluorescence intensity as a function of positive LiCl gradients imposed on SUV of DMPC. SUV of DMPC (50 mg lipid/ml) were prepared in 0.01 M Tris buffer (pH 7) with carboxyfluorescein (50 mM) entrapped in their cavity at self-quenching concentrations as described in Materials and Methods. The bulk phase carboxyfluorescein was removed by gel filtration on a Sepharose CL 4B column presaturated with 50 mM NaCl. Fluorescence intensities were measured at 35°C with an Aminco SPF-500 spectrofluorimeter (excitation at 480 nm, emission at 515 nm). Since the fluorescence intensity was linearly related to carboxyfluorescein concentration over the concentration range 10^{-8} to $3 \cdot 10^{-5}$M, carboxyfluorescein concentrations are plotted rather than fluorescence intensities. The dashed line represents the expected carboxyfluorescein concentration calculated for the release of the total amount of entrapped carboxy fluorescein.

cles at room temperature but otherwise under the same experimental conditions as described above, no fluorescence intensity increase was observed with increasing salt gradient (data not shown). This indicates that at room temperature no shrinkage of DMPC vesicles was produced by positive salt gradients consistent with FFEM results (cf. Fig. 1B).

When SUV of DMPC prepared in buffer containing 3 M LiCl and 50 mM carboxyfluorescein were exposed to a negative LiCl gradient of $\Delta C = -2.5$ M no increase in fluorescence intensity was detected. This indicates that under conditions of swelling, SUV of DMPC did neither break nor did carboxyfluorescein leak out from the internal vesicle cavity. The chromophore concentration was chosen such that dilution of the fluorescent label by water influx into the vesicle cavity is insufficient to produce an increase in fluorescence intensity. As a control, when sufficient sodium cholate was added to the DMPC vesicles to a final DMPC/cholate mole ratio of 0.5 the maximum fluorescence intensity was observed consistent with the entire release of the entrapped carboxyfluorescein.

Discussion

The results of the size analysis of DMPC-SUV by FFEM is consistent with published data [25]. The Weibull distribution describes satisfactorily the size distribution of DMPC-SUV produced by ultrasonication (cf. Tenchov et al., Ref. 12). SUV of DMPC produced by ultrasonication are fairly stable or metastable for days when stored at low temperatures (0–4°C), but aggregate and/or fuse when stored at or close to the lipid phase transition temperature of T_c = 23°C. If SUV of DMPC were prepared in buffer containing high concentrations of LiCl (> 1 M), the vesicles had a higher tendency to aggregate and/or fuse at room temperature as evident from the appearance of a visible precipitate within 1 or 2 days.

The effects of positive and negative salt gradients on SUV of DMPC and EPC (average size 20–25 nm) were determined by FFEM, EPR spin labeling and fluorescence spectroscopy. The main conclusion of the data presented is that SUV of both phospholipids are osmotically active and respond to both positive ($\Delta C > 0$) and negative salt gradients ($\Delta C < 0$). Our results are at variance with previous reports [5,8] that small unilamellar lipid vesicles with a diameter smaller than approx. 80 nm are osmotically insensitive. Positive salt gradients of LiCl produce shrinkage and/or collapse to flattened disks, while negative salt gradients make the vesicles swell. This is true at temperatures below and above the crystal-to-liquid crystal transition of the phospholipid, but not at the crystal-to-liquid crystal transition temperature. FFEM and fluorescence spectroscopic evidence show that SUV of DMPC are osmotically insensitive at this temperature (Fig. 1A and B). It was shown before that phospholipid bilayers exhibit a maximum in their lateral compressibility at the crystal-to-liquid crystal transition temperature due to the coexistence of patches of phospholipid molecules in the crystalline and liquid crystalline state [17]. It was reported that the transition state of the bilayer is associated with a marked increase in the permeability of ions [18,19] and small molecules such as sugars [20]. Furthermore it was shown that macromolecules such as proteins can be inserted in the phospholipid bilayer at this temperature [21]. The observed osmotic insensitivity of phospholipid vesicles at this temperature is probably due to the increased bilayer permeability leading to the rapid dissipation of salt gradients.

In the presence of excess LiCl in the external medium, i.e., in the presence of positive salt gradients ($\Delta C > 0$), the spherical unilamellar vesicles shrink and eventually collapse to disks. FFEM evidence shows that these disks can aggregate to stacks. Size analysis of the resulting disks indicates that single disks result from the collapse of the original spherical vesicles while stacked disks originate from fused vesicles (Fig. 3). This result indicates that shrinkage of vesicles is accompanied by fusion of the original SUV. The occurrence of disk stacking is less pronounced at high LiCl concentrations, $\Delta C > 1$ M (Fig. 3). This salting-in effect is probably due to Li^+ ions interacting with the phosphatidylcholine bilayer giving rise to positive sur-

face potentials and electrostatic repulsion between SUV [22].

Some details concerning the shrinking and swelling process of SUV in the presence of salt gradients are derived from EPR spin labeling and fluorescence spectroscopy. The results obtained with these two spectroscopic methods taken together indicate that labels entrapped in the vesicle cavity leak out during shrinkage of the vesicles induced by positive LiCl gradients. Most of the entrapped Tempocholine and carboxyfluorescein, 80% or more is released in the presence of positive LiCl gradients $\Delta C \geq 1$ M (cf. Figs. 4 and 7). A comparison of the Tempocholine (Fig. 4) and carboxyfluorescein data (Fig. 7) with the CAT 16 results shown in Fig. 5 indicates that vesicles do not break and equilibrate with the external medium during shrinkage. This comparison also clearly shows that there is an efflux of Tempocholine rather than an influx of ascorbate. Such an influx of reducing agent would produce a similar reduction of the signal intensity of the CAT 16 label as observed for the Tempocholine label (cf. Figs. 4 and 5). This is clearly not the case: the CAT 16 EPR signal intensity is reduced to about 50% in response to positive LiCl gradients. The CAT 16 experiments summarized in Fig. 5 provide evidence that some loss of EPR signal intensity occurs even in the absence of reducing agent. This loss of about 20% of the signal intensity observed in the absence of ascorbate may arise from spin exchange due to clustering (patching) of CAT 16 molecules. As shown schematically in Fig. 8 the collapse of spherical vesicles to disks leads to flat

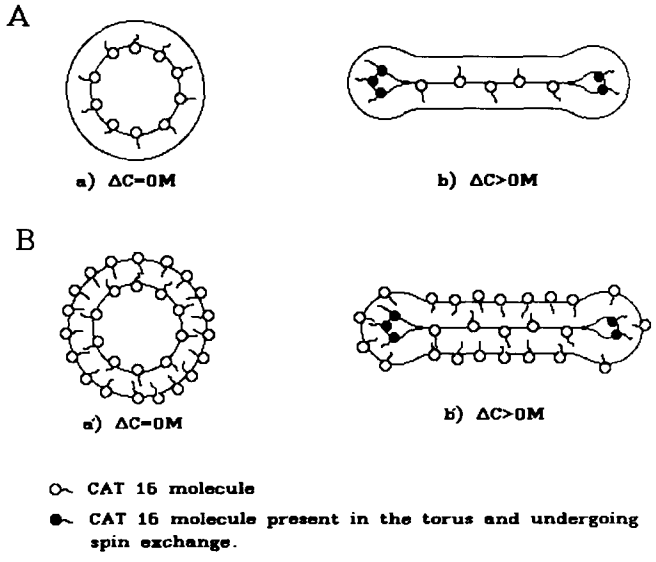

Fig. 8. Schematic diagram showing the collapse of spherical lipid vesicles labeled with CAT 16 as a result of osmotic shrinkage (A) in the presence and (B) in the absence of sodium ascorbate (0.13 M). Also shown is the possible clustering of the spin label in the torus of the disks.

as well as highly curved regions of the bilayer, and differently shaped molecules will have a preference for one or the other. As a result the spin label may be enriched in one region or the other of the disk, e.g., the torus region of the disk, giving rise to a spin exchange line. The spectral component due to spin exchange is apparently not accounted for in our determination of signal intensities by line height measurement. In the absence of a reducing agent the loss in signal intensity due to clustering of the label is approx. 20% of the total label, whereas in the presence of ascorbate a 50% reduction is observed. Bearing in mind that the EPR signal intensity observed in the presence of excess ascorbate arises from CAT 16 molecules present in the internal monolayer and considering that in SUV of DMPC about 2/3 of the phospholipid molecules are located in the outer and 1/3 in the inner layer of the bilayer, it is calculated that a 50% loss of spin label in the inner monolayer is equal to approx. 20% loss referred to the total number of spin label molecules originally present in the vesicle bilayer. This consideration lends support to the notion that the loss in signal intensity is due to clustering of spin label molecules in the inner layer of the bilayer. The clustering is apparently induced by the shape transformation sphere to disk.

From a comparison of the EPR results in Figs. 4 and 5 with those of Fig. 6 it is clear that SUV of DMPC prepared in buffer containing high LiCl concentrations behave differently from DMPC-SUV prepared in buffer without additional salt. DMPC-SUV prepared in buffer containing 4 M LiCl apparently shrink when exposed to the same medium, i.e., at $\Delta C = 0$. Figs. 6A and B show that maximum EPR signals are observed at $\Delta C = -1.5$ M and that this kind of vesicles are under osmotic stress at $\Delta C > -1.5$ M. This suggests that the vesicle cavity of SUV prepared in the presence of high salt concentrations is solute-depleted, i.e., $[LiCl]_{inside} = 4$ M is the nominal, but not real LiCl concentration. A similar phenomenom was reported for multilamellar vesicles [15]. Taking into account that 12 water molecules are bound per phosphatidylcholine head group [23] and that around the same number is required for LiCl hydration [24], the maximum amount of LiCl that can be entrapped in the cavity of SUV of DMPC is calculated to be [LiCl] = 2.5 M. This calculation is based in a vesicle diameter of 20 nm, a bilayer thickness of 4 nm and a molecular area of 0.50 nm^2 [16], with 2/3 of the DMPC molecules being located on the external and 1/3 in the internal layer of the vesicle bilayer. The prediction of this simple calculation is borne out by experiment. Maximum EPR signal intensities are observed when the DMPC-SUV are dispersed in buffer containing 2.5 M LiCl instead of 4 M LiCl (Figs. 6A and B).

Furthermore, a comparison of the data in Figs. 4 and 5 with those of Fig. 6 shows that vesicles prepared in buffer with high LiCl shrink differently from vesicles prepared in ordinary buffer. The data in Fig. 6 are consistent with FFEM showing that vesicles containing high LiCl concentrations in their cavity shrink only partially but do not totally collapse to disks. The efflux of water is probably counteracted by the hydration of the entrapped LiCl. As a result Tempocholine efflux is reduced compared to vesicles with no LiCl entrapped (cf. Figs. 4 and 6A) and at the same time ascorbate influx appears to be increased (cf. Figs. 5 and 6B). As mentioned before, the presence of LiCl appears to stabilize phosphatidylcholine SUV. This kind of stabilization is due to encapsulated LiCl and is different from the salting-in effect mentioned above.

The swelling experiments with DMPC-SUV containing carboxyfluorescein in their cavity indicate that vesicles do not break and equilibrate with the external medium during swelling: no increase in fluorescence intensity was observed. The data presented here indicate that phosphatidylcholine SUV are resistant to osmotic pressure in the sense that the bilayer integrity is maintained. Furthermore the data of Figs. 6A and B provide evidence that swelling of DMPC-SUV spin-labeled with either Tempocholine or CAT 16 is accompanied with a significant reduction of both spin labels. This probably indicates that the influx of water during swelling is coupled with an influx of ascorbate reducing the spin label present in the internal cavity.

Acknowledgements

We are grateful to Dr. P. Schurtenberger for writing the computer program used to analyse the bar histograms in terms of a Weibull distribution. This work was partly supported by the Swiss National Science Foundation (Grant 31-25719.88).

Appendix

If the torus shown in the schematic diagram (Fig. 8) of a collapsed vesicle or disk is ignored and complete collapse of the vesicle is assumed to take place, at least to a first approximation, a relationship between the length $2l + 2d$ (Fig. 9) of the disk derived from FFEM and the diameter Φ of the original, spherical vesicle can be derived. The general expression of the volume of a disk is:

$$V = \pi \int_a^b f^2(x)\,dx$$

In the diagram of Fig. 9 the thickness of the disk is $2d$ and its length is $2l + 2d$. With these parameters the

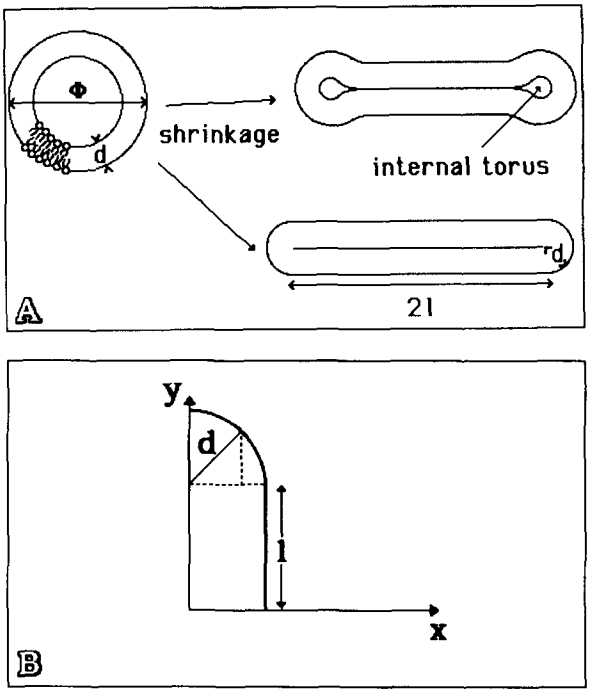

Fig. 9. (A) Schematic diagram showing the collapse of spherical lipid vesicles as a result of osmotic shrinkage. B: Function used for the calculation of disc volumes.

volume of the disk V_{disk} is:

$$V_{disk} = 2\pi \int_0^d [l^2 + d^2 - x^2 + 2l(d^2 - x^2)^{1/2}]\,dx$$

$$f(x) = (d^2 - x^2)^{1/2} + l$$

Integration yields:

$$V_{disk} = 2\pi dl^2 + 4\pi/3d^3 + \pi^2 d^2 l$$

Assuming to a first approximation that the actual bilayer volume remains constant upon transformation of vesicles to disks then:

$$V_{disk} = (4\pi/3)[(\Phi/2)^3 - (\Phi/2 - d)^3]$$

Inserting appropriate values for d into the above equation and solving for l yields for collapsed DMPC-SUV ($d = 4$ nm):

$$l = -58.5 + 0.706\Phi$$

and for collapsed EPC-SUV ($d = 4.6$ nm):

$$l = -67.0 + 0.705\Phi$$

These equations were used to transform l derived from values measured from electron micrographs to the original diameter Φ of the spherical vesicle.

References

1 Bystrov, V.F., Shapiro, Yu.E., Viktorov, A.V., Barsukov, L.I. and Bergelson, L.D. (1972) FEBS Lett. 25, 337–338.
2 De Kruijff, B., Cullis, P.R. and Radda, G.K. (1975) Biochim. Biophys. Acta 406, 6–20.
3 Lichtenberg, D., Peterson, N.O., Girardet, J.-L., Kainosho, M., Kroon, P.A., Seiter, C.H.A., Feigenson, G.W. and Chan, S.I. (1975) Biochim. Biophys. Acta 382, 10–21.
4 Hauser, H. (1989) Proc. Natl. Acad. Sci. USA 86, 5351–5355.
5 Johnson, S.M. and Buttress, N. (1973) Biochim. Biophys. Acta 307, 20–26.
6 Bangham, A.D., De Gier, J. and Greville, G.D. (1967) Chem. Phys. Lipids 1, 225–246.
7 Deamer, F. and Bangham, A.D. (1976) Biochim. Biophys. Acta 443, 629–634.
8 Milon, A., Lazrak,T., Albrecht, A.-M., Wolff, G., Weill, G., Ourisson, G. and Nakatani, Y. (1986) Biochim. Biophys. Acta 859, 1–9.
9 Müller, M., Meister, N. and Moor, H. (1980) Balzers report BB 800 011 DE.
10 Müller, M., Marti, T. and Kriz, S. (1980) in Electron Microscopy, 7th European Congress on Electron Microscopy Foundations, Vol. 2, pp. 720–732, Leiden.
11 Marsh, D. and Watts, A. (1981) in Liposomes: From Physical Structure to Therapeutic Applications (Knight, C.G., ed.), pp. 139–188, Elsevier/North-Holland Biomedical Press.
12 Tenchov, B.G., Yanev, T.K., Tihova, M.G. and Koynova, R.D. (1985) Biochim. Biophys. Acta 816, 122–130.
13 Phillips, M.C., Williams, R.M. and Chapman, D. (1969) Chem. Phys. Lipids 3, 234–244.
14 Mabrey, S. and Sturtevant, J.M. (1978) Methods Membr. Biol. 9, 237–274.
15 Gruner, S.M., Lenk, R.P., Janoff, A.S. and Ostro, M.J. (1985) Biochemistry 24, 2833–2842.
16 MacDonald, R.C. and Simon, S.A. (1987) Proc. Natl. Acad. Sci. USA 84, 4089–4093.
17 Phillips, M.C., Graham, D.E. and Hauser, H. (1975) Nature 254, 154–156.
18 Papahadjopoulos, D., Jacobson, K., Nir, S. and Isac, T. (1973) Biochim. Biophys. Acta 311, 330–348.
19 Wu, S.H.W. and McConnell, H.M. (1973) Biochem. Biophys. Res. Commun. 55, 484–491.
20 Linden, C.D., Wright, K.L., McConnell, H.M. and Fox, C.F. (1973) Proc. Natl. Acad. Sci. USA 70, 2271–2275.
21 Op den Kamp, J.A.F., De Gier, J. and Van Deenen, L.L.M. (1974) Biochim. Biophys. Acta 345, 253–256.
22 Hauser, H. (1991) Chem. Phys. Lipids 57, 309–325.
23 Chapman, D., Williams, R.M. and Ladbrooke, B.D. (1967) Chem. Phys. Lipids 1, 445–475.
24 Marshall, W.L. (1986) J. Chem. Soc., Faraday Trans.1 82, 2283–2299.
25 Watts, A., Marsh, D. and Knowles, P.F. (1978) Biochemistry 17, 1792–1801.